

## Ultra Compact and Low-power TDC and TAC Architectures for Highly-Parallel Implementation in Time-Resolved Image Sensors

David Stoppa<sup>1</sup>, Fausto Borghetti<sup>1</sup>, Justin Richardson<sup>3,5</sup>, Richard Walker<sup>2,3</sup>  
Robert K. Henderson<sup>3</sup>, Marek Gersbach<sup>4</sup>, Edoardo Charbon<sup>4</sup>

<sup>1</sup>Fondazione Bruno Kessler (FBK), Trento, Italy, +390461314531, +390451302040, stoppa@fbk.eu

<sup>2</sup>STMicroelectronics Imaging Division, Edinburgh, U.K.

<sup>3</sup>The University of Edinburgh, Edinburgh, U.K.

<sup>4</sup>TU Delft, Delft, The Netherlands

<sup>5</sup>Dialog Semiconductor, Edinburgh, U.K.

**Abstract-** We report on the design and characterization of three different architectures, namely two Time-to-Digital Converters (TDCs) and a Time-to-Amplitude Converter (TAC) with embedded analog-to-digital conversion, implemented in a 130-nm CMOS imaging technology. The proposed circuit solutions are conceived for implementation at pixel-level, in image sensors exploiting Single-Photon Avalanche Diodes as photodetectors. The fabricated 32x32 TDCs/TACs arrays have a pitch of 50 $\mu$ m in both directions while the average power consumption is between 28mW and 300mW depending on the architectural choice. The TAC achieves a time resolution of 160ps on a 20-ns time range with a differential and integral non-linearity (DNL, INL) of 0.7LSB and 1.9LSB respectively. The two TDCs have a 10-bit resolution with a minimum time resolution between 50ps and 119ps and a worst-case accuracy of  $\pm 0.5$  LSB DNL and 2.4 LSB INL. An overview of the performance is given together with the analysis of the pros and cons for each architecture.

### I. Introduction

Electronic circuits aimed at time measurements have been developed for nuclear science applications since the 1960's [1] and their performance has been constantly improving, mainly thanks to the reduction of propagation delays as the fabrication CMOS technologies are progressing towards nanometer channel lengths. However, these devices are typically based on complex circuits [2]-[5], whose area occupation and power consumption makes it impossible to implement highly parallel on-chip architectures. Recent fabrication techniques for low-noise Single-Photon Avalanche Diodes (SPADs) in deep-submicron CMOS technologies, as proven in [6],[7], make it now possible to integrate a TAC/TDC inside each pixel, allowing fully parallel operation as required to realize a monolithic Time-Correlated Single-Photon Counting (TCSPC) imager. Several TAC/TDC architectures [8]-[10] have been developed and successfully implemented at pixel-level within the project MEGAFRAME [11], demonstrating the feasibility of the largest single-chip array of TACs/TDCs so far reported [13]. In this contribution a summary and comparison of these architectures is given.

### II. Time-resolved SPAD-based Pixel Architecture

The pixel developed within the MEGAFRAME project supports both time-uncorrelated and time-correlated single-photon imaging. Each pixel of the array consists of a SPAD with quenching circuitry, a TAC/TDC stage, and a memory to allow a time-interleaved readout-convert operation. Three different time-measuring architectures have been developed and fully characterized: a TDC based on an external master clock (TDC-EC) [8], a ring-oscillator TDC (RO-TDC) [10] and a TAC with embedded ADC conversion (TADC) [9].

#### A. Time-to-Amplitude-to-Digital Converter (TADC)

The schematic diagram of the TAC is shown in Figure 1. The basic cell consists of a current source (IbiasP), which charges up capacitor Cs when the switch-structure, composed of Mp1, Mp2, Mp3, and IbiasN, is turned on. The basic building block used to generate the voltage ramp is replicated into three layout-matched structures: Stage1 and Stage2 are used alternately to measure the number of events or the event arrival time in a time interleaved fashion, while StageREF is used to generate a reference voltage ramp used to implement the embedded ADC. The time-coding voltage ramp is started when a photon is detected, whilst the charging of capacitor Cs is stopped by the system clock (to map a 25-ns time range a 40-MHz frequency is used for the STOP signal). At the end of the observation window, a voltage is accumulated across capacitor Cs that is

proportional to the photon arrival time. At this point, the reference TAC block is externally stimulated by the signal CNT (globally distributed to the whole pixel matrix, synchronously with the 6-bit Gray Code Counter), while the output of TAC selector is applied to the second branch (time interleaved operation) and  $V_{O1}$  is connected to the comparator. As the number of CNT pulses increases, the voltage at node  $V_{O_{CNT}}$  increases and when it reaches the same voltage previously stored on  $V_{O1}$  the voltage comparator toggles, thus sampling the digital code GCC<0:5> into the memory.

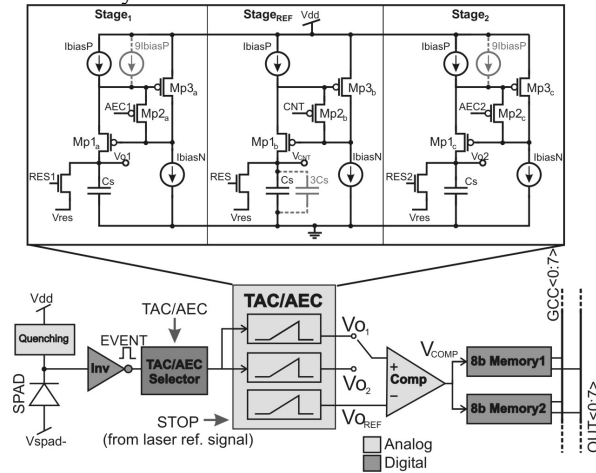


Figure 1: Schematic of the TAC with embedded digital conversion (TADC).

### B. Time-to-Digital Converter based on External Clock (TDC-EC)

This architecture exploits an external clock generated by an on-chip PLL that runs at 280MHz and is distributed to the whole TDC array as depicted in Figure 2. The global clock is then doubled at the pixel level to achieve higher resolution. Each 10-bit TDC consists of a two-level (coarse and fine) interpolator activated by the digital pulse from a SPAD upon photon detection (START signal). The coarse interpolator consists of a 6-bit ripple counter clocked by the global clock CK. The fine interpolator further divides each clock cycle by sending the START signal through a delay chain consisting of 16 buffer propagation delays. To minimize dependence on substrate and supply noise, a differential buffer architecture was chosen for the implementation of the 16-tap delay line. On the first clock edge after the START signal the propagation of the pulse through the delay chain is stopped, thus the number of buffer elements that toggled between the photon detection and the subsequent clock edge corresponds to the time elapsed between these two events. A coder converts the resulting thermometer code of the fine interpolator output into a 4-bit binary number and the result is stored in one of the two 10-bit memories to allow the read out of the pixel array in parallel with the acquisition of the following frame.

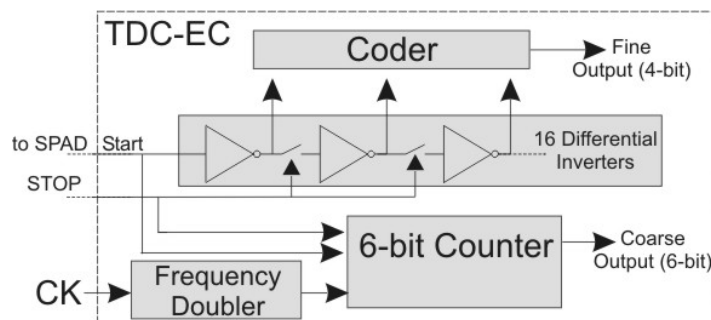


Figure 2: Block diagram of the TDC-EC.

### C. Ring-Oscillator Time-to-Digital Converter (RO-TDC)

In this case the clock is internally generated by means of a ring-oscillator realized by four differential buffers and activated by the START signal (see Fig. 3). Similarly to the TDC-EC architecture, coarse conversion is achieved by means of a 7-bit ripple counter while the fine conversion is provided by the dynamic state stored in the internal nodes of the ring (3 bits). The use of a 'power of 2' number of elements simplifies the fine state binary

coding, while positive feedback in the ring is achieved by simply swapping the polarity of feedback on the last stage.

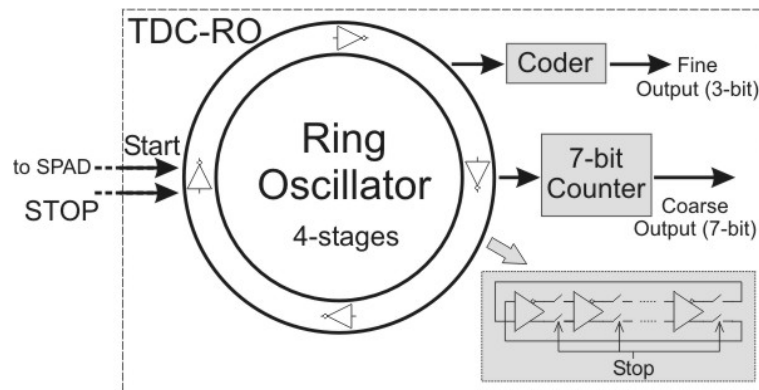


Figure 3: Block diagram of the RO-TDC.

The differential buffers have an NMOS supply regulation to reduce the impact of power supply noise. The propagation delay of the buffers can be adjusted by tuning the gate-voltage of the NMOS transistors controlling the tail current, by means of a calibration loop locking the mean array time resolution to a stable external clock source using a PLL-like structure.

### III. Experimental Results and Comparison

The three versions have been implemented in a 32x32-pixel array and fabricated in a 130-nm CMOS technology (die micrograph of the RO-TDC version is shown in Figure 4). The three pixel-arrays share the same SPAD front-end, readout circuitry and I/O padding in order to allow a direct comparison of the performance.

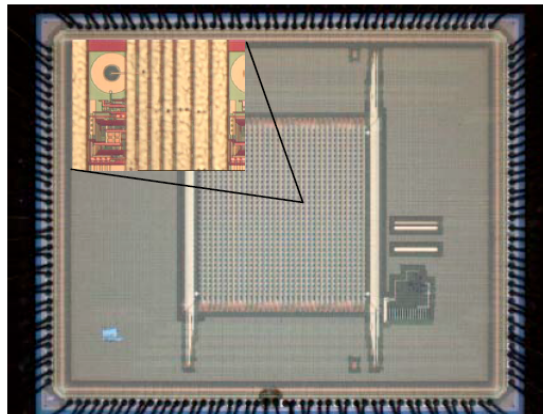


Figure 4: 32x32-pixel array with in-pixel TDC.

More details concerning the three structures and the characterization procedure are provided in [8-10], while a summary of the performance achieved by the three architectures is given in Table I.

In light of the results obtained from the testing of the implemented TAC/TDC architectures it is possible to draw the following conclusions:

*TADC*: The main advantage of this architecture, basically exploiting the charge of a capacitor by means of a constant current source, is that its time resolution performance is not limited by the use of deep-submicron technologies, so the proposed design can be easily ported to less-advanced fabrication processes without substantial degradation effects [12], and only minor impact onto the area occupation. On the other hand, to achieve good uniformity in the implementation of large array of TACs, the basic TAC circuit is unsuitable, and the architecture proposed here adds complexity to cope with mismatch effects. This was also needed because to achieve the high frame rate of 1Mfps targeted by the MEGAFRAME project the only viable solution was to stream digital data directly from the chip, thus requiring on-chip high-speed analog-to-digital conversion. In this

case our choice was to adopt a pixel-level ADC approach, and to exploit it to realize a TAC with embedded digital conversion exhibiting good immunity to mismatch effects.

Table I: Performance summary of the TAC/TDC arrays.

PARAMETER	TAC [9]	TDC-EC [8]	TDC-RO [10]	Unit
Bit resolution	6	10	10	bits
Time resolution (LSB)	160	119	178/52	ps
Uniformity	$\pm 2$	$\pm 2$	8	LSB
INL	1.9	$\pm 1.2$	$\pm 0.4/1.4$	LSB
DNL	0.7	$\pm 0.4$	$\pm 0.5/2.4$	LSB
Time Jitter	< 600	185	107/32	ps @ FWHM
Power Consumption	300	94	28/38	$\mu\text{W}@$ 500kframe/sec

Another key point of the TAC structure is that the time range can be adjusted by simply changing the reference current used to charge up the capacitors, while in a TDC this is limited by the clock-frequency and the counter depth.

From Table I it is evident that the main drawbacks of this architecture with respect to TDCs are higher power consumption, mainly due to the extra-bias current (IBIASN in Fig. 1) needed by the high-bandwidth switches, and the worst jitter noise performance of the three versions, although this figure is dominated by the FPGA jitter noise contribution and can be considered as a worst case estimation of the TAC noise on the whole time-range. On the other hand for the TDCs a refined characterization procedure has been used. In any case it is reasonable to expect a higher jitter noise for the TADC because of the extra contribution given by the relatively low-slope ramp used for the analog-to-digital conversion. Another contribution to the TADC power dissipation is due to the distribution of the Gray-code signals to the whole pixel-array, as required to implement the analog-to-digital conversion.

Finally, the uniformity along the 32x32-pixel array is quite good in comparison to TDCs although there is no calibration loop implemented in the TADC. This has been achieved thanks to the use of the in-pixel reference stage, which dramatically improves the immunity to process mismatch.

*TDC-EC* and *RO-TDC*: These structures provide excellent performance in this deep-submicron technology implementation both in terms of timing resolution and area occupation. The TDC-EC could potentially be integrated in a very compact structure, however, to successfully distribute the global clock over a large TDC-array there is an intrinsic limitation in the maximum clock frequency, which requires a local frequency doubler and a longer delay line chain with respect to the RO-TDC, where a higher clock frequency can be used being locally generated. The use of a global clock will also impact the total power consumption. As can be seen in Table I, the TDC-EC consumes more power with respect to the RO-TDC, because of the “ $CV^2f$ ” dissipation due to the distribution network. On the contrary the RO-TDC is very power efficient when the number of active TDCs is low, which is the typical operating condition in FLIM applications. Moreover the local ring oscillator in the RO-TDC could run at very high frequency, providing the best time resolution (52ps) among the three structures, while still exhibiting the lowest power consumption. There are two main design issues to be taken into account in the implementation of the RO-TDC: the first one concerns the potential metastability of the structure, which has been solved by implementing a hysteresis output stage, the other one is the periodic INL error intrinsic of this structure, which has been attenuated by means of an optimized layout of the four stages in order to keep each stage perfectly symmetric (analog approach).

The main drawback of the RO-TDC, at least in our implementation where the structure has been implemented in a very compact layout (less than  $50 \times 50 \mu\text{m}^2$ ), is the relatively high DNL-INL. Additionally, for longer conversion periods, oscillator based jitter is permitted to accumulate for longer periods of time.

On the basis of the above mentioned considerations the final version of the MEGAFRAME sensor, consisting of a 160x128-pixel array has been based on the RO-TDC version. Even in such a massive parallel TDCs implementation, spread on a very large area sensor ( $8 \times 6.4 \text{mm}^2$ ), this approach confirmed its validity as demonstrated by the excellent results summarized in [13].

#### IV. Conclusions

Three different time-measurement circuit architectures have been designed and fabricated within a 130-nm CMOS technology. A Time-to-Amplitude Converter with embedded analog-to-digital conversion and two Time-to-Digital Converters have been described. The TDCs implement two different strategies for the reference clock, the first one using an external clock globally distributed to the whole TDC-array, the second one generating the clock locally by means of a ring-oscillator in each pixel. The fabricated 32x32 TDCs/TACs arrays have a pitch of 50 $\mu$ m in both directions and share the very same front-end and read out electronics to allow a direct comparison of the performance. A summary of most important parameters and the analysis of the pros and cons for each architecture has been given. The resulting time-correlated pixel array is a viable candidate for single photon counting (TCSPC) applications such as fluorescent lifetime imaging microscopy (FLIM), nuclear or 3D imaging and permits scaling to larger array formats.

#### References

- [1] R. Nutt, "Digital Time Intervalometer", *The Review of Scientific Instruments*, 1968, Vol. 39, Issue 9.
- [2] J.-P. Jansson, et al., "A CMOS time-to-digital converter with better than 10 ps single-shot precision", *IEEE J. Solid-State Circuits*, vol. 41, no.6, pp. 1286-1296, June 2006.
- [3] A. S. Yousif et al., "A Fine Resolution TDC Architecture for next generation PET imaging", *IEEE Trans. on Nuclear Science*, vol. 54, no. 5, pp. 1574-1582, Oct. 2007.
- [4] M. Lee, et al., "A 9b, 1.25ps Resolution Coarse-Fine Time-to-Digital Converter in 90nm CMOS that Amplifies a Time Residue", *Digest of IEEE Symposium on VLSI Circuits*, pp. 168-169, 2007.
- [5] P. Chen, et al., "A low-cost low-power CMOS time-to-digital converter based on pulse stretching", *IEEE Trans. on Nuclear Science*, vol. 53, no. 4, pp. 2215-2220, Aug. 2006.
- [6] C. Niclass et al., "A single photon avalanche diode implementation in 130-nm CMOS technology", *IEEE J. of Sel. Top. in Quantum Electron.*, vol. 13, pp. 863-869, 2007.
- [7] J. A. Richardson et al., "Low Dark Count Single-Photon Avalanche Diode Structure Compatible With Standard Nanometer Scale CMOS Technology", *IEEE Photonics Technology Letters*, Vol. 21, Issue 14, pp. 1020-1022, (2009).
- [8] M. Gersbach et al., "A Parallel 32x32 Time-to-Digital Converter Array Fabricated in a 130nm Imaging CMOS Technology", *IEEE European Solid-State Circuits Conference (ESSCIRC'09)*, pp. 196-199, Sept. 2009.
- [9] D. Stoppa et al., "A 32x32-Pixel Array with In-Pixel Photon Counting and Arrival Time Measurement in the Analog Domain", *IEEE European Solid-State Circuits Conference (ESSCIRC'09)*, pp. 204-207, Sept. 2009.
- [10] J. Richardson et al., "A 32x32 50ps Resolution 10 bit Time to Digital Converter Array in 130nm CMOS for Time Correlated Imaging", *IEEE Custom Integrated Circuits Conference (CICC'09)*, pp. 77-80, Sept. 2009.
- [11] EC FET Open MEGAFRAME project, [www.megaframe.eu](http://www.megaframe.eu).
- [12] D. Stoppa, L. Pancheri, M. Scandiuozzo, L. Gonzo, G.-F. Dalla Betta, A. Simoni, "A CMOS 3-D Imager based on Single Photon Avalanche Diode", *IEEE Trans. On Circuits and Systems I*, Vol. 54, No. 1, January 2007.
- [13] C. Veerappan, J. Richardson, R. Walker, D.-U. Li, M. W. Fishburn, Y. Maruyama, D. Stoppa, F. Borghetti, M. Gersbach, R. K. Henderson, E. Charbon, "A 160x128 Single-Photon Image Sensor with On-Pixel 55ps 10b Time-to-Digital Converter", *IEEE International Solid-State Circuits Conference*, San Francisco, CA, USA, vol. 54, 2011, pp. 312-313, 20-24 February 2011.